N1 and N3 Linkage Isomers of Neutral and Deprotonated Cytosine with *trans*-[$(CH_3NH_2)_2Pt^{II}$]**

Wolfgang Brüning,[a] Eva Freisinger,[a] Michal Sabat,[b] Roland K. O. Sigel,[a] and Bernhard Lippert*[a]

Dedicated to Professor Karl Wieghardt on the occasion of his 60th birthday

Abstract: A series of complexes obtained from the reaction of *trans*-[$(CH_3NH_2)_2Pt^{II}$] with unsubstituted cytosine (CH) and its anion (C), respectively, has been prepared and isolated or detected in solution: *trans*-[Pt(CH_3NH_2)$_2$(CH-*N3*)Cl]Cl · H_2O (**1**), *trans*-[Pt(CH_3NH_2)$_2$(CH-*N3*)$_2$](ClO_4)$_2$ (**1a**), *trans*-[Pt(CH_3NH_2)$_2$(C-*N3*)$_2$] · 2H_2O (**1b**), *trans*-[Pt(CH_3NH_2)$_2$(CH-*N3*)$_2$](ClO_4)$_2$ · 2DMSO (**1c**), *trans*-[Pt(CH_3NH_2)$_2$(CH-*N1*)$_2$](NO_3)$_2$ · 3H_2O (**2a**), *trans*-[Pt(CH_3NH_2)$_2$(C-*N1*)$_2$] · 2H_2O (**2b**), *trans*-[Pt(CH_3NH_2)$_2$(CH-*N1*)(CH-*N3*)](ClO_4)$_2$ (**3a**), *trans*-[Pt(CH_3NH_2)$_2$(C-*N1*)(C-*N3*)] (**3b**), and *trans*-[Pt(CH_3NH_2)$_2$(*N1*-C-*N3*)(*N3*-C-*N1*)Cu(OH)]ClO_4 · 1.2H_2O (**4**). X-ray crystal structures of all these compounds, except **3a** and **3b**, are reported. Complex **2a** is of particular interest in that it contains the rarer of the two 2-oxo-4-amino tautomer forms of cytosine, namely that with the N3 position protonated. Since the effect of Pt^{II} on the geometry of the nucleobase is minimal, bond lengths and angles of CH in **2a** reflect, to a first approximation, those of the free rare tautomer. Compared to the preferred 2-oxo-4-amino tautomer (N1 site protonated) of CH, the rare tautomer in **2a** differs particularly in internal ring angles ($7-11\,\sigma$). Formation of compounds containing the rare CH tautomers on a preparative scale can be achieved by a detour (reaction of Pt^{II} with the cytosine anion, followed by cytosine reprotonation) or by linkage isomerization (N3 → N1) under alkaline reaction conditions. Surprisingly, in water and over a wide pH range, N1 linkage isomers (**3a**, **2a**) form in considerably higher amounts than can be expected on the basis of the tautomer equilibrium. This is particularly true for the pH range in which the cytosine is present as a neutral species and implies that complexation of the minor tautomer is considerably promoted. Deprotonation of the rare CH tautomers in **2a** occurs with pK_a values of 6.07 ± 0.18 ($1\,\sigma$) and 7.09 ± 0.11 ($1\,\sigma$). This value compares with pK_a 9.06 ± 0.09 ($1\,\sigma$) (average of both ligands) in **1a**.

Keywords: bioinorganic chemistry · nucleobases · platinum · tautomerism

Introduction

Theoretically, neutral cytosine can exist in six tautomeric forms. If different orientations of the enol and the imino protons are considered as well, the number of possible structures is fourteen.[1] According to ab initio calculations,[2] at least in the gas phase, the two 2-hydroxo-4-amino forms I and II are slightly more stable (≈ 0.8 kcal mol^{-1}) than the 2-oxo-4-amino form III, which appears to be preferred in the solid state and in solution.[3] The second 2-oxo-4-amino tautomer IV is about 7 kcal mol^{-1} less stable than I and II, thereby representing a truly minor tautomer of cytosine. The predominance of the hydroxo-amino tautomer(s) is confirmed by IR spectroscopy under matrix isolation conditions at 15 K.[4] Only these four tautomers are shown in Scheme 1.

As we have demonstrated in a number of cases,[5] metal ion binding can be applied to stabilize rare nucleobase tautomers normally present in extremely low concentrations, and to crystallize them in their metal-complexed forms in reasonable yields. With an understanding of the effects of a metal ion on the geometry of a heterocyclic ligand[6] and with precise X-ray crystal structural data of the metal complex, an estimation of the geometry of the rare nucleobase tautomer can be

[a] Prof. Dr. B. Lippert, Dr. W. Brüning, Dr. E. Freisinger, Dr. R. K. O. Sigel
Fachbereich Chemie
Universität Dortmund, 44221 Dortmund (Germany)
Fax: (+49) 231-755-3797
E-mail: lippert@pop.uni-dortmund.de

[b] Dr. M. Sabat
Department of Chemistry
University of Virginia
Charlottesville, Virginia 22901 (USA)

[**] Metal-Stabilized Rare Tautomers of Nucleobases, Part 7. For Part 6, see: ref. [5f]

Supporting information for this article is available on the WWW under http://www.chemeurj.org/ or from the author.

  0947-6539/02/0820-4681 $ 20.00+.50/0

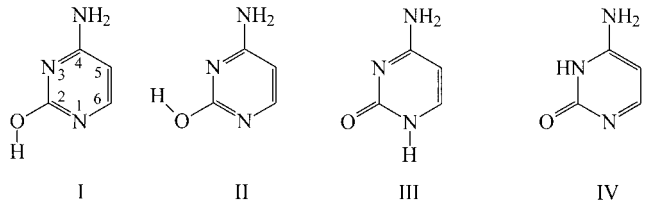

Scheme 1.

made,[5a,b] thereby enabling a comparison with data derived from quantum chemical calculations.

We decided to study Pt^{II} complex formation with unsubstituted cytosine and its monoanion, respectively, for several reasons: 1) the list of metal complexes of cytosine with a confirmed X-ray structure is relatively short; [7–13] in fact, for Pt^{II} there are only two examples known.[13] 2) With very few exceptions (O2 binding of Ni^{II},[9a] N3,O2 bridging of $[Rh^{II}]_2$,[9b] N1 and N1,N4 binding of CH_3Hg^{II}[11, 14]) metal attachment is always through N3. Specifically, full X-ray data of a N1-bound complex is not available.[14] Provided N1 linkage isomers are obtained, they should present a rich potential for molecular recognition reactions that take advantage of the availability of O2, N3, and N4 as H bonding sites. 3) We eventually wanted to explore whether N1,N3 dimetalated complexes of cytosine could be assembled into cyclic compounds of defined structures, similar to the situation with uracil anions, with which we have prepared open molecular boxes.[15]

As a start, we decided to study in detail the complex forming properties of cytosine with a *trans*-diamineplatinum(II) species, *trans*-$[Pt(CH_3NH_2)_2(H_2O)_2]^{2+}$. Here we report the syntheses, X-ray structures, and the solution behavior of N1 and N3 cytosine linkage isomers.

Results and Discussion

Observation of linkage isomers on the ^{1}H NMR scale: According to ^{1}H NMR spectroscopy, reaction of *trans*-$[(CH_3NH_2)_2Pt^{II}]$ with cytosine in D_2O (pH* 5.7, 40 °C, 96 h, Pt:CH 1:3) yields a multitude of products, especially in the initial phase of the reaction. The large number of resonance siganls can be rationalized if the formation of different stoichiometries (Pt:cytosine = 1:1, 1:2, 2:1), linkage isomerism (N1, N3, N1/N3 and/or other patterns), and in the case of 1:2 complexes the possibility of rotational isomerism are considered. After long reaction times and with an excess of CH, essentially only 1:2 complexes are to be expected. For these, three different species—Pt(CH-*N3*)$_2$, Pt(CH-*N1*)$_2$, Pt(CH-*N3*)(CH-*N1*)—are possible, each of which could exist as pairs of rotamers (*head*–*head*, *hh*, or *head*–*tail*, *ht*). Most of the resonances were assigned after isolation of the compounds, and by pH-dependent NMR spectra (vide infra). Figure 1 shows a typical spectrum (aromatic protons only).

Five intensive sets of H6 and H5 doublets, two of the latter strongly overlapping, were identified and were correlated by a ^{1}H,^{1}H COSY experiment (see Supporting Information). These are assigned to unreacted cytosine (CH) and to two rotamers of the bis(cytosine) complexes containing the N3 linkage isomers **1a** and the mixed N1,N3 linkage isomers **3a** each (see below for the assignment of the latter). Under the conditions of the experiment, formation of the N1 linkage isomer **2a** is hardly detectable. Only a very weak doublet at $\delta = 8.03$ (insert in Figure 1) can be assigned to this species. Its H5 counterpart is buried under the other H5 doublets.

X-ray structures of 1, 1a, 1c, and 2a: Crystallographic data for **1**, **1a**, **1b**, **1c**, **2a**, **2b**, and **4** are given in Table 1. Figures 2 and 3 show the cations of *trans*-$[Pt(CH_3NH_2)_2(CH\text{-}N3)Cl]Cl \cdot H_2O$ (**1**), *trans*-$[Pt(CH_3NH_2)_2(CH\text{-}N3)_2](ClO_4)_2$ (**1a**), and *trans*-$[Pt(CH_3NH_2)_2(CH\text{-}N1)_2](NO_3)_2 \cdot 3H_2O$ (**2a**), as well as *trans*-

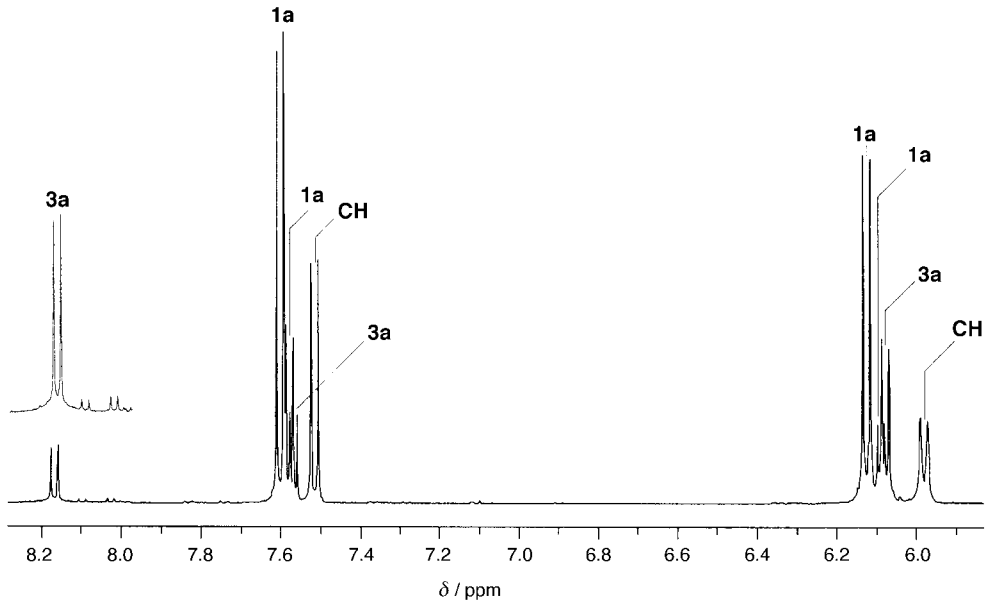

Figure 1. Section of a ^{1}H NMR spectrum (400 MHz, D_2O, aromatic region only) of a reaction mixture of cytosine (90 mM) and *trans*-$[Pt(CH_3NH_2)_2(D_2O)_2]^{2+}$ (30 mM) after 96 h at 40 °C, pH* 5.7.

0947-6539/02/0820-4682 $ 20.00+.50/0 *Chem. Eur. J.* **2002**, *8*, No. 20

Table 1. Crystallographic data for **1**, **1a**, **1b**, **1c**, **2a**, **2b**, and **4**.

	1	**1a**	**1b**	**1c**	**2a**	**2b**	**4**
formula	$C_6H_{17}N_5O_2Cl_2Pt$	$C_{10}H_{20}N_8O_{10}Pt$	$C_{10}H_{22}N_8O_4Pt$	$C_{14}H_{32}N_8O_{12}S_2Cl_2Pt$	$C_{10}H_{26}N_{10}O_{11}Pt$	$C_{10}H_{22}N_8O_4Pt$	$C_{10}H_{21.4}N_8O_{8.2}ClCuPt$
asym. unit	$C_6H_{17}N_5O_2Cl_2Pt$	$C_5H_{10}N_4O_5Pt_{0.5}$	$C_5H_{11}N_4O_2Pt_{0.5}$	$C_7H_{16}N_4O_6SClPt_{0.5}$	$C_5H_{13}N_5O_{5.5}Pt_{0.5}$	$C_5H_{11}N_4O_2Pt_{0.5}$	$C_5H_{10.7}N_4O_{4.1}Cl_{0.5}Cu_{0.5}Pt_{0.5}$
fw	457.23	339.17	256.73	417.29	328.75	256.72	339.51
crystal system	monoclinic	monoclinic	monoclinic	monoclinic	triclinic	monoclinic	monoclinic
space group	$P2_1/c$	$P2_1/c$	$P2_1/c$	$P2_1/c$	$P\bar{1}$	$P2_1/c$	$C2/m$
a[Å]	6.360(2)	6.581(1)	8.526(2)	10.127(2)	7.775(2)	8.411(2)	16.7364(6)
b[Å]	26.917(9)	20.495(4)	12.645(3)	13.110(3)	8.368(1)	12.761(3)	14.2511(5)
c[Å]	7.745(3)	7.908(2)	8.115(2)	11.578(2)	9.490(2)	7.847(2)	11.0388(4)
α[°]					65.29(1)		
β[°]	94.11(2)	106.07(3)	116.05(3)	101.77(3)	80.60(1)	110.42(3)	117.625(3)
γ[°]					76.09(1)		
V[Å^3]	1322(1)	1024.9(4)	786.0(3)	1504.8(5)	543.0(2)	789.3(3)	2332.7(2)
Z	4	4	4	4	2	4	8
T[K]	173	293	293	293	293	293	91
$\lambda(Mo_{K\alpha})$[Å]	0.71069	0.71069	0.71069	0.71069	0.71069	0.71069	0.71069
ρ[g cm^{-3}]	2.296	2.198	2.169	1.842	2.011	2.160	1.93
μ[mm^{-1}]	10.966	7.174	8.961	5.043	6.535	8.923	7.042
transm. coeff.	0.599–1.000	0.215–0.343	0.999–0.628	0.365–0.560	0.999–0.685	0.999–0.503	0.65–1.00
2θ range [°]	4.0–46.0	9.6–51.3	5.4–60.0	9.5–51.4	4.7–48.0	5.2–54.0	3.0–54.3
no. reflns collected	2076	1912	3799	5546	1838	1836	7816
no. reflns observed[a]	1317	1259	1457	1773	1687	1208	1742
no. of param.	145	178	150	223	180	144	158
$R1$ (obs. data)[b]	0.0263	0.0270	0.0180	0.0240	0.0237	0.0252	0.044
wR_2 (obs. data)[c]	0.0358	0.0606	0.0378	0.0388	0.0587	0.0607	0.065
$(\Delta/\rho)_{min}$[e Å^{-3}]	−0.84	−1.724	−0.748	−0.982	−0.934	−1.871	−0.58
$(\Delta/\rho)_{max}$[e Å^{-3}]	0.81	1.000	0.524	0.344	0.699	1.964	1.60

[a] Observation criterion for **1**, **4**: $I > 3\sigma(I)$; for **1a**, **1b**, **1c**, **2a**, **2b**: $F_o > 4\sigma(F_o)$. [b] $R1 = \Sigma||F_o| - |F_c||/\Sigma|F_o|$. [c] For **1**, **4**: $R_w = [\Sigma w(|F_o| - |F_c|)^2/\Sigma w(|F_o|^2)]^{1/2}$; for **1a**, **1b**, **1c**, **2a**, **2b**: $wR_2 = [\Sigma w(F_o^2 - F_c^2)^2/\Sigma w(F_o^2)^2]^{1/2}$.

$[Pt(CH_3NH_2)_2(CH\text{-}N3)_2](ClO_4)_2 \cdot 2DMSO$ (**1c**). In **1**, **1a**, and **1c** the predominant oxo-amino tautomer III of cytosine is coordinated to Pt through N3, whereas in **2a** it is the rare oxoamino tautomer IV, that is bound to Pt through N1 (vide infra). In the two bis(cytosine) compounds **1a** and **2a**, which were crystallized from an aqueous solution, the two bases adopt *head–tail* orientations. This feature even holds up for *trans*-$[Pt(CH_3NH_2)_2(CH\text{-}N3)_2](ClO_4)_2 \cdot 2DMSO$ (**1c**), which had been isolated from DMSO instead of H_2O. The reason for also crystallizing **1a** from a DMSO solution resulted from our previous findings on the influence of the solvent in the stabilization of different rotamer forms of bis(nucleobase) complexes of *trans*-$[a_2Pt^{II}]$ ($a = NH_3$ or CH_3NH_2).[16, 17] Specifically, we had shown that with *trans*-$[Pt(CH_3NH_2)_2(1\text{-MeC-}N3)_2]^{2+}$ (with 1-MeC = 1-methylcytosine) DMSO stabilizes the *head–head* rotamer in solution, whereas water stabilizes the *head–tail* form.[16a] While we were able to show the same effect in solution for the CH analogue, the solid-state structure of **1c** reveals that, if H bonding of DMSO is intermolecular, the two bases may still adopt a *head–tail* orientation (Figure 3).

Table 2. Bond lengths [Å] and angles [°] for free cytosine and cytosine in the Pt complexes **1**, **1a**, **1c** and **2a**.

	Cytosine[a]		**1**	**1a**	**1c**	**2a**
	Anhydrous	Monohydrate				
N1–C2	1.381(3)	1.371(2)	1.39(1)	1.374(7)	1.368(5)	1.355(7)
C2–N3	1.364(3)	1.350(2)	1.38(1)	1.385(7)	1.381(5)	1.374(7)
C2–O2	1.241(3)	1.251(2)	1.23(1)	1.216(7)	1.224(4)	1.234(6)
N3–C4	1.336(3)	1.341(2)	1.33(1)	1.345(7)	1.355(4)	1.351(7)
C4–C5	1.410(3)	1.425(2)	1.41(1)	1.420(9)	1.408(5)	1.404(7)
C4–N4	1.342(3)	1.326(2)	1.34(1)	1.334(8)	1.315(5)	1.310(7)
C5–C6	1.340(3)	1.333(2)	1.33(1)	1.342(10)	1.314(6)	1.347(8)
C6–N1	1.353(3)	1.353(2)	1.34(1)	1.329(8)	1.354(5)	1.365(7)
C6-N1-C2	121.9(2)	121.5(2)	123.1(8)	123.9(6)	122.1(5)	118.3(4)
N1-C2-N3	118.2(2)	119.6(2)	116(1)	116.2(5)	117.6(4)	117.8(5)
N1-C2-O2	119.5(2)	118.5(2)	121.5(9)	121.4(5)	121.2(4)	122.6(5)
N3-C2-O2	122.2(2)	121.9(2)	123(1)	122.4(6)	121.1(5)	119.6(5)
C2-N3-C4	119.4(2)	119.1(2)	121.9(9)	120.8(5)	119.6(3)	124.8(5)
N3-C4-C5	122.7(2)	121.7(2)	121(1)	120.6(5)	120.8(4)	116.7(5)
C5-C4-N4	120.2(2)	120.2(2)	120(1)	120.4(6)	120.7(4)	123.7(5)
N3-C4-N4	117.1(2)	118.1(2)	119(1)	119.0(6)	118.5(3)	119.6(5)
C4-C5-C6	117.0(2)	117.5(2)	118(1)	117.8(6)	118.5(4)	118.0(5)
C5-C6-N1	120.8(2)	120.5(2)	120(1)	120.6(7)	121.1(4)	124.3(5)

[a] Ref. [18].

Pt–N bond lengths and angles about the Pt centers are not unusual and compare well with related compounds containing N-bonded nucleobases and the *trans*-$[(CH_3NH_2)_2Pt^{II}]$ fragment, respectively.[16] A detailed comparison of the geometries of the cytosine rings in the bis(cytosine) complexes **1a**, **1c**, and **2a** (Table 2) to that of free cytosine[18] reveals the following: 1) the internal ring angles at the respective non-coordinating ring N atoms (N1 in **1**, **1a** and **1c**, N3 in **2a**) are consistent with these sites carrying protons, which thus rules out any 2-hydroxo tautomer structures (I, II). In the latter

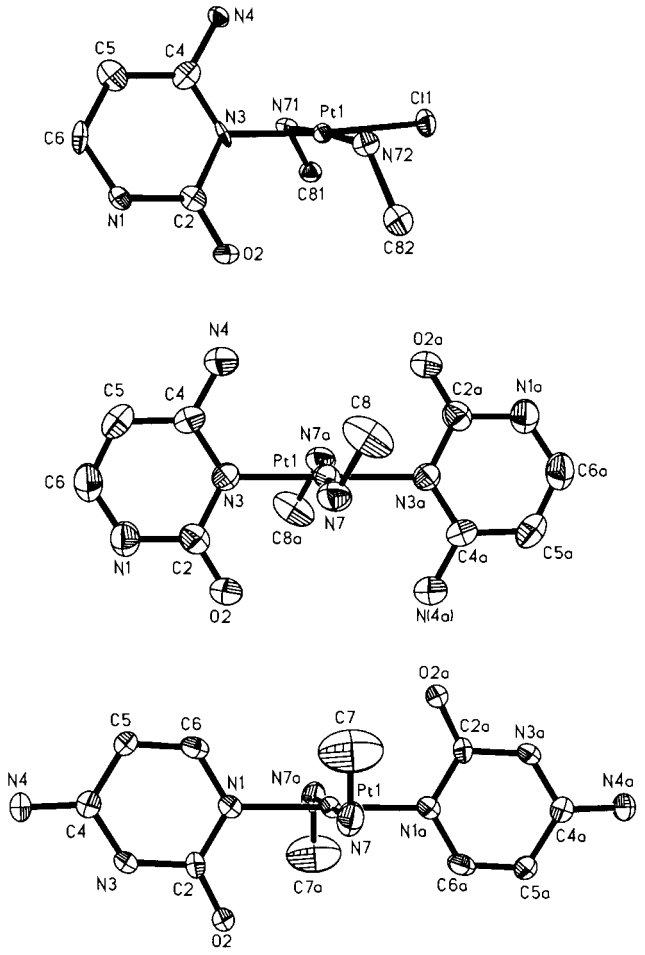

Figure 2. Cations of *trans*-$[Pt(CH_3NH_2)_2(CH\text{-}N3)Cl]Cl\cdot H_2O$ (**1**), *trans*-$[Pt(CH_3NH_2)_2(CH\text{-}N3)_2](ClO_4)_2$ (**1a**), and *trans*-$[Pt(CH_3NH_2)_2(CH\text{-}N1)_2](NO_3)_2\cdot 3H_2O$ (**2a**) with atom numbering schemes (from top to bottom).

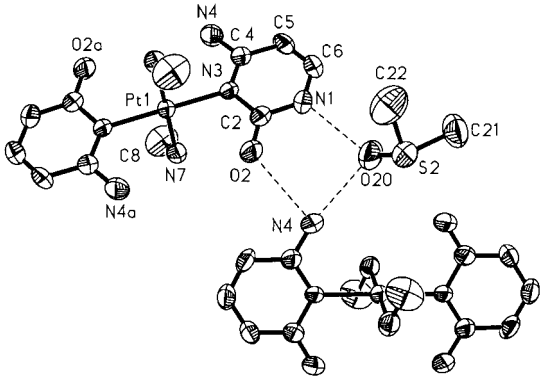

Figure 3. Section of solid-state structure of *trans*-$[Pt(CH_3NH_2)_2(CH\text{-}N3)_2](ClO_4)_2\cdot 2$DMSO (**1c**) with H bonds between the DMSO molecule and two cations indicated.

case, these angles should be well below 120°. Intermolecular H bonding patterns (see below) are in agreement with this conclusion. 2) Ring geometries of **1a** and **1c** do not differ significantly, as expected. 3) The N3 and N1 linkage isomers essentially differ in nucleobase angles only: internal ring angles at N3 are larger in **2a** than in **1a** and **1c** ($6-9\sigma$[19]), whereas the opposite is true for the internal ring angles at N1 (max. 8σ). The other two angles that display differences are N3-C4-C5 (larger by $6-7\sigma$ in **1a** and **1c**) and C5-C6-N1 (larger by $4-5\sigma$ in **2a**). Both angles affected are at the C atoms adjacent to the metal binding site; excluding C2, however. 4) Compared to the solid-state structures of cytosine (anhydrous or monohydrate), which represent tautomer III, there are no significant changes in bond lengths in **1**, **1a** and **1c**, and the differences in angles do not exceed the 3σ level. These statements are true even if structural parameters of N1-substituted neutral cytosines[20] are included. Taken together, this means that the ring geometry of tautomer III is only insignificantly altered upon binding of Pt^{II} to N3, at least on the basis of the accuracy of the structures of **1a** and **1c**. This conclusion is also supported by findings in other Pt^{II} nucleobase systems.[5a,b] 5) A comparison of CH (major tautomer III, anhydrous or monohydrate) with CH rings in **2a** (minor tautomer IV, platinated) reveals a trend to shorter N1–C2 (max. 3.4σ) and shorter C4–N4 bond lengths (max. 4.2σ) in **2a**. The shortening of the C4–N4 bond is certainly consistent with the N3 site being protonated. In addition, there are considerable differences in angles. Of the internal ring angles, the largest difference exists for N3-C4-C5 (smaller in **2a** by max. 6°, 11σ), followed by C2-N3-C4 (larger in **2a** by max. 5.4°, 10σ), C6-N1-C2 (smaller in **2a** by max. 3.6°, 8σ), and C5-C6-N1 (larger in **2a** by max. 3.8°, 7σ). External ring angles at C2 and C4 likewise differ somewhat ($5-6\sigma$); however, this feature should not be over-emphasized. The calculated geometry of tautomer IV in the gas phase[3] agrees reasonably well with the geometry of the cytosine ring in **2a** as far as ring angles are concerned. This even refers to the tilting of the exocyclic NH_2 group of cytosine toward N3H (C5-C4-N4, 123.7(5)° in **2a**, 125.5° in IV). On the other hand, agreement of cytosine bond lengths in **2a** and the calculated structure of the uncomplexed rare tautomer is generally poor, with deviations of up to 0.07 Å.

Hydrogen bond formation: Hydrogen bonding in the solid state reveals direct contacts between adjacent cations in all four structures. In **1** cations are arranged in infinite chains along the crystallographic *x* axis connected through one H bond between O2 and one amine group (2.96(1) Å, Figure 1, Supporting Information), respectively. The motif found in **1a** is very similar. Again, the cations form infinite chains along *x*, this time involving both carbonyl oxygens and both amine groups in hydrogen bonding (2.995(8) Å, Supporting Information). In **1c**, a structure consisting of parallel layers can be observed. Those layers, stretched in the *y*,*z* direction, are built up by cations connected through O2···N4–H bonds (2.943(4) Å, Figure 3, and Supporting Information) and bridging DMSO molecules (N1···O20 2.724(5) Å, N4···O20 2.848(5) Å). In **2a**, the bases of adjacent cations are involved in base pairing (two N3···O2 bonds each, 2.820(8) Å) forming infinite chains along the *z* axis (Figure 4). Two water molecules participate in base pairing, joining the carbonyl and amino group (N4···O1w 2.871(9) Å, O1w···O2 2.775(7) Å). The interbase H-bonding pattern, seen in **2a**, is remarkable in that it illustrates how, in principle, cytosinium cations (N3-protonated) could self-associate in an alternative way to that with anions, as typically seen in cytosinium salts.[21] Moreover, it can be envisaged that upon hemi*de*protonation

0947-6539/02/0820-4684 $ 20.00+.50/0 *Chem. Eur. J.* **2002**, *8*, No. 20

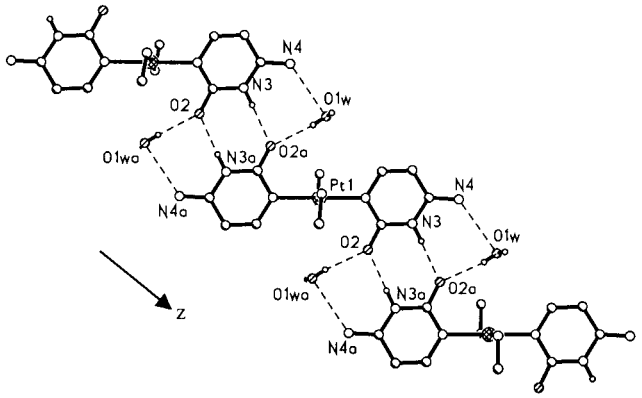

Figure 4. Association of cations of **2a** through pairwise H-bond formation (2.820(6) Å) leading to infinite chains along the *z* axis.

of this CH – CH pair and a slight shift of the two cytosine rings, a situation is realized which is structurally analogous to that of hemiprotonated cytosine,[22] displaying three hydrogen bonds between two cytosine rings.

Comparison of ^{1}H NMR spectra of 1:2 complexes 1a and 2a: There are three major differences between the two linkage isomers **1a** and **2a**. 1) The number of resonances: the N3 linkage isomer **1a** displays two sets of cytosine H5 and H6 doublets in D_2O, in a ratio of approximately 1:3. The two sets of resonances are attributed to *head – head* and *head – tail* rotamers, with the latter preferred (see also below). The situation thus is very similar to that of the corresponding 1-MeC-*N3* complex.[16a] In contrast, the N1 linkage isomer **2a** gives rise to single sets of H5 and H6 doublets in the ^{1}H NMR spectrum and likewise to a single ^{195}Pt NMR signal. We assume that rotation about the Pt–N1 bond, because of the presence of a single exocyclic group, only (O2) is sufficiently fast with **2a**, resulting in simpler spectra. Similarly, in [D_6]DMSO only a single set of H5 and H6 doublets is observed for **2a** (Supporting Information). In contrast, the amino protons are split in a 1:1 ratio ($\delta = 7.35$ and 8.58). This feature appears to be a consequence of hindered rotation of the $N4H_2$ group as a consequence of an increase in the double bond character of the C4–N4 bond as a result of protonation at N3. 2) Chemical shifts of the cytosine protons: H5 resonances of the two rotamers of **1a**, as well as that of **2a**, occur in a relatively narrow range close to the corresponding resonance of free cytosine. H6 resonances of **1a** are also close to that of H6 in cytosine, shifted somewhat to lower field. Only H6 of **2a** and H6 of the N1-bound cytosine in **3a** are well-separated from all other cytosine resonances and occur furthest downfield, in the $\delta = 8 - 8.2$ range. 3) ^{195}Pt coupling: from previous ^{1}H NMR work,[13a] we had expected to detect ^{195}Pt,^{1}H coupling (^4J between ^{195}Pt and H5 in the case of N3 coordination, and ^3J coupling with H6 in the case of N1 metal binding). However, because of the use of high-field instruments,[23] ^{195}Pt satellites were usually not visible. The only ^{195}Pt coupling clearly resolved was that between Pt and the CH_3 resonance of the methylamine ligands ($^3J \approx 38$ Hz). Moreover, in the D_2O spectrum of **2a**, satellites of the H6 doublet are visible, yet not resolved to the same extent as previously shown by us.[13a]

Selected chemical shifts of **1a** and **1b** as well as of their deprotonated forms are listed in Table 3.

Rotational isomerism of 1a: As mentioned, *trans*-[$Pt(CH_3NH_2)_2(CH\text{-}N3)_2$]($ClO_4$)$_2$ (**1a**) occurs in aqueous solution in a mixture of *head – tail* and *head – head* rotamers. When solid **1a** is dissolved in D_2O, equilibrium is reached

Table 3. ^{1}H and ^{195}Pt NMR chemical shifts of **1a**, **1b**, **2a**, and **2b** in D_2O.[a]

	H5	H6	^{195}Pt	pH*
1a	6.13 (*ht*)	7.61 (*ht*)	– 2643 (*ht*)	5.9
	6.08 (*hh*)	7.58 (*hh*)	– 2594 (*hh*)	
1b	5.95	7.69	–	12.1
2a	6.09	8.10	– 2559	1.7
2b	5.91	7.93	–	12.3

[a] ^3J (H5,H6) $\approx$ 7.1 Hz each.

within minutes. The more intense resonance signals are from the *head – tail* species. In the ^{195}Pt NMR spectrum, two resonance signals of different intensities are also observed at $\delta = -2643$ (*ht*) and $\delta = -2594$ (*hh*). As with the analogous 1-methylcytosine compound,[16a] it is remarkable to see that the two species, which have identical donor atoms and differ in relative ligand orientation only, give rise to ^{195}Pt NMR resonances which are 50 ppm apart. Similar splittings of ^{195}Pt NMR signals, albeit much smaller in magnitude (6 – 14 ppm), have occasionally been reported also for complexes of *cis*-[a_2Pt^{II}], for example, in [Pt(en)(5′-dAMP-*N7*)$_2$] (5′-dAMP = 2-deoxyadenosine 5′-monophosphate)[24] and [$Pt(Me_2ppz)G_2$] (Me_2ppz = N,N′-dimethylpiperazine; G = various guanine derivatives).[25] Signal splitting in these systems has been assigned to Δ and Λ forms of the *ht* rotamers[24] and *hh* and *ht* isomers,[25] respectively.

Time-dependent ^{1}H NMR spectra of **1a** dissolved in [D_6]DMSO reveal that the original *head-tail* species interconverts into the *head – head* species and that equilibrium is reached within $\approx$3 h at 22 °C. The ratio of *hh*:*ht* is then $\approx$9:1 (Figure 5).

As pointed out above, despite the preference of the *head-head* rotamer in DMSO solution, the product that crystallizes from DMSO again displays a *head – tail* arrangement of the two bases (compound **1c**).

pH*-Dependent ^{1}H NMR spectra of 1a and 2a: From the pD-dependent ^{1}H NMR spectra (H5 and H6 chemical shifts versus pD), only a single pK_a value for the two sequential (de)protonation steps of N1 position of **1a** is deduced whereas for its linkage isomer **2a**, two pK_a values for the deprotonation of N3 could be calculated. Thus for the N3 linkage isomer **1a**, pK_a values of 9.17 ± 0.09 (1 σ) (*ht* rotamer), and 9.00 ± 0.07 (1 σ) (*hh* rotamer) for deprotonation of the N1 positions are obtained; these two values are the same within their error limits, giving an averaged pK_a 9.06 ± 0.09 (1 σ) (weighted mean). The two rotamers of **1a** do not behave differently, as had been the case in a bis(1-methyluracil) complex of [(tmeda)Pt^{II}],[26] where differences in the stabilization of protonated species are possible for steric reasons. With the assumption that there is no mutual influence of the NH sites

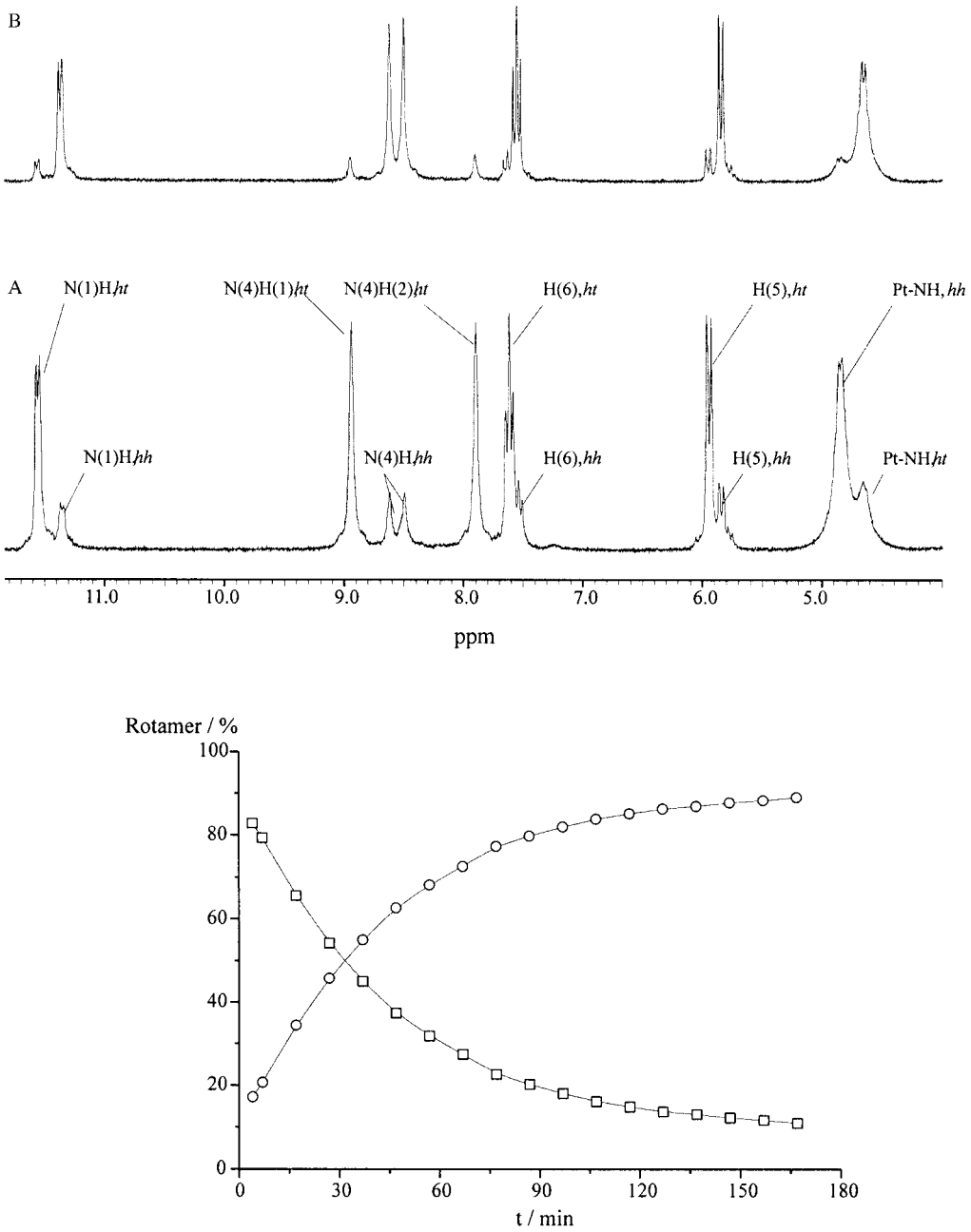

Figure 5. Section of a ^{1}H NMR spectra of **1a** in [D$_6$]DMSO at 22 °C: A) 10 min after sample preparation, and B) 15 h later. The time dependence of the rotamer distribution of **1a** at 22 °C is given in the lower part (□ *ht*, ○ *hh*).

upon subsequent stepwise deprotonation, a difference in microacidity constants of 0.6 is to be expected for the two cytosine bases in **1a**,[27] hence individual pK_a values should be about p$K_{a1} \approx 9.4$ and p$K_{a2} \approx 8.8$. For [PtCl$_3$(CH-*N3*)]$^-$, a drop in pK_a from 12.15[28] to 9.4,[13a] hence an acidification by approximately 2.8 log units, had previously been determined. The higher acidities of N3-platinated cytosine nucleobases in **1a** are most likely a consequence of the dipositive charge of **1a** as compared to the negative charge of [PtCl$_3$(CH-*N3*)]$^-$. For complex **2a**, the situation is a bit more complicated in that the change in chemical shifts of H6 from the pD-dependent ^{1}H NMR experiments can be fitted with equations that take either one or two pK_a values into account (Figure 6a). The first gives a pK_a value of 6.73 ± 0.05 (1σ), whereas in the latter case, values of 6.07 ± 0.18 (1σ) and 7.09 ± 0.11 (1σ) are obtained. Although the errors are larger when taking two separated pK_a values into account, the fit of the experimental data is better (reflected by a smaller error-square-sum, factor of 5). The ΔpK_a of ≈ 1 is slightly larger than the statistically expected one of 0.6, which would be obtained if the two deprotonation sites are truly independent. This finding can easily be explained by the change in overall charge of complex **2a** upon the first deprotonation from 2+ to 1+ leading to a lower acidity of the second deprotonation step. A further reason might be the formation of CH–C homo basepairs, which are expected to lead to the formation of long chains and could have a stabilizing effect on the intermediate singly deprotonated form.

0947-6539/02/0820-4686 $ 20.00+.50/0 *Chem. Eur. J.* **2002**, *8*, No. 20

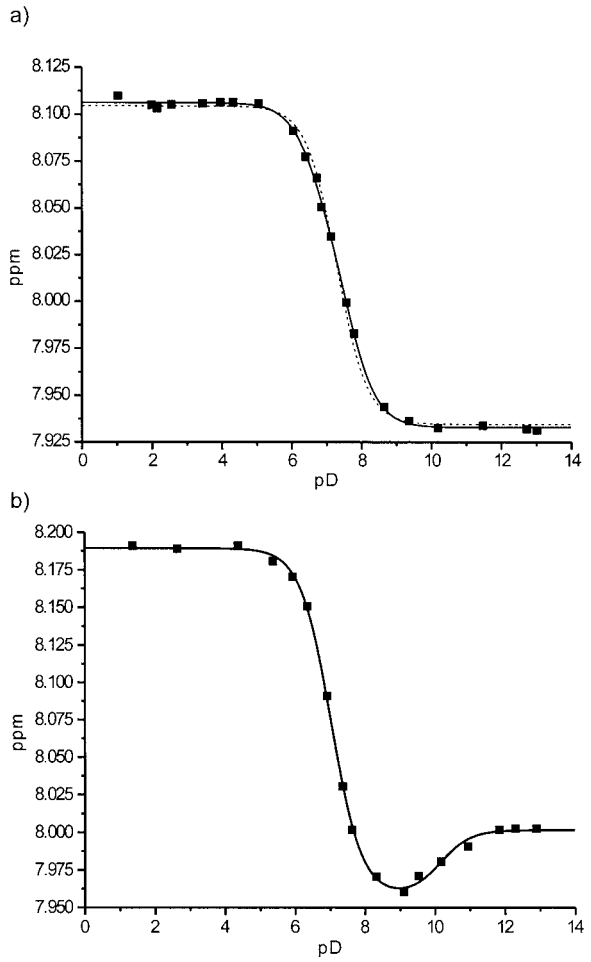

Figure 6. a) pD dependence of the H6 chemical shifts of *trans*-$[Pt(CH_3NH_2)_2(CH\text{-}N1)_2](NO_3)_2 \cdot 3H_2O$ (**2a**). The solid line represents the fit taking two pK_a values into account (6.07 ± 0.18 (1σ) and 7.09 (1σ)), whereas the dashed line is the fit with only one $pK_a = 6.73 \pm 0.05$ (1σ) (see also text). b) pD dependence of the H6 chemical shifts of *trans*-$[Pt(CH_3NH_2)_2(CH\text{-}N1)(CH\text{-}N3)](ClO_4)_2$ (**3a**) with the calculated fit of the experimental data, giving pK_a values of 6.48 ± 0.05 (1σ) and 9.55 ± 0.12 (1σ).

^{1}H NMR spectra provided no evidence for any additional deprotonation step ($N4H_2$) of the cytosine ligands in **1a** and **2a** up to pH* 13.

Lowfield resonance signals: The three doublets in the range $\delta = 8.0-8.2$ of the D_2O spectrum (Figure 1) are assigned to H6 resonance signals of N1-platinated cytosine species from a comparison with **2a** (see above). At least the doublet furthest downfield is of sufficient intensity to unambiguously determine its pD dependence (Figure 6b). The pK_a value of 6.48 ± 0.05 (1σ) clearly identifies it as belonging to a Pt(CH-*N1*) species. There is, however, an important difference between this resonance and that of **2a**, in that the former displays a second $pK_a = 9.55 \pm 0.12$ (1σ) (Figure 6b). We propose that this can be attributed to the N1-bound cytosine in the mixed-linkage isomer *trans*-$[Pt(CH_3NH_2)_2(CH\text{-}N1)(CH\text{-}N3)]^{2+}$ (**3a**) and that following deprotonation of the N1-bonded cytosine ($pK_a = 6.48$), deprotonation of the N3-bonded cytosine ($pK_a = 9.55$) influences the *trans*-positioned (C-*N1*) ligand as well, and hence its H6 resonance (Scheme 2).

The H6 doublet of the N1-bound cytosine of **3a** has its H5 counterpart at $\delta = 6.08$ (^{1}H,^{1}H COSY). A second H6 doublet of an intensity comparable to that of the $\delta = 8.16$ doublet is identified at $\delta = 7.57$, in the range typical of N3-bound cytosine. Its H5 counterpart coincides with the signal of the N1-bound cytosine at $\delta = 6.08$ (^{1}H,^{1}H COSY), thereby doubling the intensity of this doublet. This interpretation is also in agreement with a linkage isomerization experiment described below.

The two weak doublets between $\delta = 8$ and 8.1 are not assigned with certainty to specific N1-bound species, although their pD dependence is consistent with this binding pattern. It appears that one of the two weak signals could be assigned to a rotamer of **3a** or to **2a**.

Relative abundance of mixed tautomer complex 3a and of the N1 linkage isomer: The cytosine tautomer III (Scheme 1) is the preferred one in the condensed phase and it has been estimated that in aqueous solution it exceeds the second most abundant tautomer IV by a factor of almost 1000.[2a] However, it is noted that, upon reaction with *trans*-$[(CH_3NH_2)_2Pt^{II}]$, the species distribution in slightly acidic D_2O (Figure 1) does not reflect this situation, and that the mixed N1,N3 isomer **3a** is formed to an extent that greatly exceeds the natural abundance of tautomer IV. As stated above, there is even the chance that one of the two weak H6 resonances between $\delta = 8.0$ and 8.1 can be attributed to **2a** with two (CH-*N1*) ligands bound to Pt^{II}. In fact, this phenomenon is seen over a wide pH range ($\approx 2-10$), and it is also confirmed with [(dien)Pt^{II}] (dien = diethylenetriamine).[29] The simplicity of the latter system—only N1, N3 and mixed N1/N3 species are formed and they are identified on the basis of the pH* dependence of their ^{1}H NMR chemical shifts—permits a direct estimation of linkage isomer abundances. It is found that the N3 linkage isomer always forms preferentially, yet it exceeds the N1 linkage isomer only by a factor of 10–20, depending on the reaction conditions (pH, ratio Pt^{II}:cytosine).[29, 30] It needs to be emphasized that this observation is of particular significance in the pH range where cytosine exists in its neutral form ($\approx$pH 6–10) and hence the tautomer equilibrium of cytosine is relevant. What it implies is that a minor tautomer, estimated to be present in an abundance of less than 10^{-3} relative to the preferred one, is "titrated out" by a metal species to an extent which increases its abundance in complexed form $\approx$100-fold. Any preference for a particular donor site is less surprising when cytosine is present as an anion (high pH), hence when both N1 and N3 positions are deprotonated and the term tautomerism becomes obsolete. Similar arguments apply to the pH range in which cytosine is protonated, provided protonation occurs with overwhelming preference at N3, as is generally assumed.

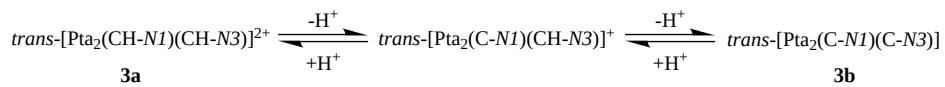

3a **3b**

Scheme 2.

Effects of Pt binding sites on ligand acidity: Neutral cytosine is present in aqueous solution predominantly in the 2-oxo-4-amino tautomer form III. The macro acidity constant for deprotonation of cytosine is $10^{-12.15}$ ($pK_a = 12.15$).[28] This value essentially corresponds to that of the predominant tautomer III. In **1a** this proton becomes more acidic by 3.1 log units (average of two pK_a values of **1a**). It is unlikely that deprotonation of the exocyclic amino group takes place to a measurable extent considering the high pK_a value of this group (≈ 16.7).[31] If Pt^{II} is bound to N1 (compound **2a**), the N3H proton has a pK_a of 6.07 ± 0.18 (1σ) and 7.09 ± 0.11 (1σ), respectively (see above). This means that placing a Pt^{II} entity in the N1 position of cytosine and shifting the proton to N3 increases the acidity of this proton almost a million fold (factor $10^{5.6}$) as compared to free cytosine (c.f. macroacidity constant $10^{-12.15}$). On the other hand, comparison with protonated cytosine (CH_2^+, pK_a 4.58)[28] reveals the expected decrease in ligand acidity (2 log units) upon substitution of the N1H by Pt^{II}.

The situation with N1- and N3-linkage isomer complexes of cytosine contrasts with that found for the corresponding complexes of the uracil monoanion. There the increase in the acidity of the platinated monoanion (UH) is virtually identical for the two binding sites: $pK_a = 11.4$ for N1H in N3–Pt, and $pK_a = 11.5$ for N3H in N1–Pt.[32] In the absence of bound Pt^{II}, the pK_{a2} for uracil is 14.2,[33] meaning an increase in ligand acidity by ≈ 2.8 log units upon Pt binding. Conversely, replacement of a proton of the neutral uracil by a Pt^{II} entity reduces the acidity of uracil by 1.7 log units, from 9.7 in the free ligand to 11.4–11.5 in the two UH–Pt linkage isomers. If, in a more elaborate treatment, microacidity constants for the formation of the individual uracil anion tautomers[34] are considered (≈ 9.4 for N3 deprotonation, ≈ 10.0 for N1 deprotonation),[35] the reduction in acidity amounts to 11.5–9.4 = 2.1 log units for the N1 linkage isomer and to 11.4–10.0 = 1.4 log units for the N3 linkage isomer.

X-ray structures of 1b and 2b: The structures of the neutral complexes *trans*-$[Pt(CH_3NH_2)_2(C\text{-}N3)_2]\cdot 2H_2O$ (**1b**) and *trans*-$[Pt(CH_3NH_2)_2(C\text{-}N1)_2]\cdot 2H_2O$ (**2b**) are given in Figure 7. While similar to **1a** and **2a**, as far as the *head-tail* arrangement of the nucleobases and the Pt coordination spheres are concerned, there are also distinct differences between the four compounds. For example, the Pt–N(cytosine) bond length in the N1 linkage isomer **2b** is shorter than in the N3 linkage isomer **1b** ($\Delta = 0.019(4)$ Å, 4.75σ), within the cytosine the N1–C2 bond is longer in **2b** (0.047(7) Å, 7σ), and there is a trend to a longer C5–C6 bond in **1b** (0.024(8) Å, 3σ) (Table 4). The only slight difference in angles refers to an exocyclic one (N3-C2-O2; trend to larger value in **2b** by $1.6(5)^\circ$, 3σ); however, it could be influenced by crystal packing. It thus appears that deprotonation of the two platinated tautomers markedly levels off structural differences seen between **1a** and **1c** on one hand and **2a** on the other (c.f. above). The only significant exception is the N1–C2 bond.

In both compounds, ring deprotonation (N1 in **1b**, N3 in **2b**) is evident from the large decrease in ring angles as compared to the complexes carrying neutral cytosine tautomers (**1a**, **1c**, **2a**). The largest difference (6.5°, 10σ) is between **1a** and **1b**.

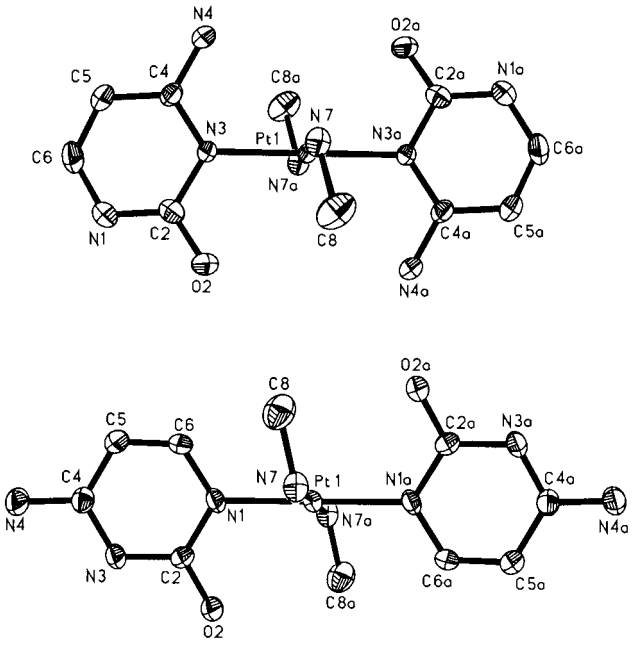

Figure 7. Views of *trans*-$[Pt(CH_3NH_2)_2(C\text{-}N3)_2]\cdot 2H_2O$ (**1b**) (top) and *trans*-$[Pt(CH_3NH_2)_2(C\text{-}N1)_2]\cdot 2H_2O$ (**2b**) (bottom).

Table 4. Comparison of bond lengths [Å] and angles [°] of deprotonated cytosine ligands in linkage isomers **1b** and **2b**.

	1b	**2b**
N1–C2	1.340(4)	1.387(6)
C2–N3	1.401(4)	1.384(6)
C2–O2	1.268(4)	1.250(5)
N3–C4	1.363(4)	1.347(6)
C4–C5	1.398(5)	1.400(6)
C4–N4	1.339(4)	1.337(6)
C5–C6	1.340(5)	1.316(6)
C6–N1	1.344(5)	1.365(6)
C6-N1-C2	117.4(3)	116.9(4)
N1-C2-N3	121.9(3)	120.5(4)
N1-C2-O2	120.3(3)	120.2(4)
N3-C2-O2	117.7(3)	119.3(4)
C2-N3-C4	118.1(3)	119.2(4)
N3-C4-C5	119.9(3)	120.6(4)
N3-C4-N4	118.7(3)	117.8(4)
C5-C4-N4	121.5(3)	121.7(5)
C4-C5-C6	117.7(3)	118.2(4)
C5-C6-N1	124.5(3)	124.0(4)

The packing patterns and H bonding schemes of **1b** and **2b** are similar as evident from the similar cell constants. In both compounds the Pt complexes form a network in the *y* and *z* directions and are connected through H bonds between the amine groups and the N1 and N3 positions of the cytosine bases, respectively (2.990(4) and 3.047(6) Å, Supporting Information). The water molecules in each structure are strongly involved in hydrogen bonding to two donor groups ($N4H_2$) and two acceptor atoms (O2), respectively, thus explaining why it was possible to crystallographically locate and refine their protons (2.722(4)–3.089(5) Å for **1b**, 2.779(5)–3.022(6) Å for **2b**, Supporting Information).

0947-6539/02/0820-4688 $ 20.00+.50/0 *Chem. Eur. J.* **2002**, *8*, No. 20

Linkage isomerization N3 → N1: When a solution of *trans*-$[Pt(CH_3NH_2)_2(CH\text{-}N3)_2](ClO_4)_2$ (**1a**) in D_2O is brought to pH* 11.5 (to give essentially **1b**) and kept at 40 °C, the appearance of new resonances is observed as early as 60 min after sample preparation. The new resonances are attributed to an intermediate that reaches its concentration maximum after ≈1 d and subsequently diminishes again at the expense of the final product (Figure 8). The intermediate and the final

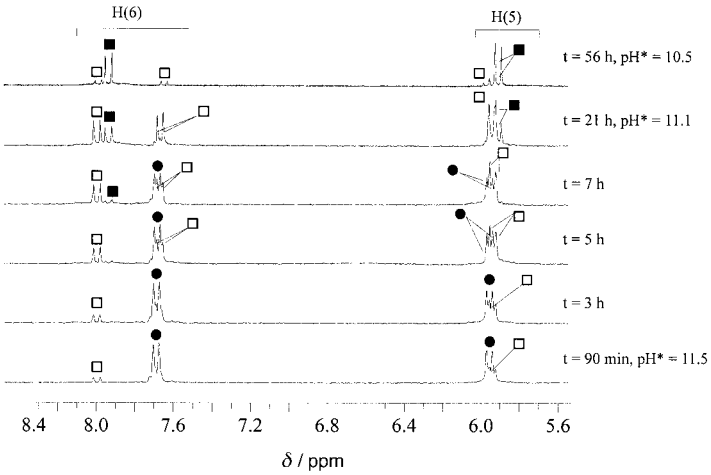

Figure 8. Time dependence of ^1H NMR spectra (low-field region only) of **1a/1b** (pH* 11.5–10.5, D_2O, 40 °C, 200 MHz) with H5 and H6 resonances of **1b** (●), of *trans*-$[Pt(CH_3NH_2)_2(C\text{-}N1)(C\text{-}N3)]$ (□), and of **2b** (■).

product are readily identified on the basis of their chemical shifts as the deprotonated form of **3a**, hence *trans*-$[Pt(CH_3NH_2)_2(C\text{-}N1)(C\text{-}N3)]$ (**3b**) and *trans*-$(CH_3NH_2)_2(C\text{-}N1)_2]$ (**2b**), respectively. The ^1H NMR spectra provide no indication that the interconversion **1b** → **3b** → **2b** takes place by a dissociative mechanism, since resonances from free cytosine are not detectable. It tentatively suggests that the linkage isomerization is an intramolecular migration process, possibly involving the migration of Pt^{II} from N3 to N1 via an O2 intermediate. Deprotonation of the CH-*N3* ligand of **1a** to give C-*N3* might indeed increase the nucleophilicity of O2 as well.

The metal migration process described here is different from that observed with the Pt^{IV} complex *trans*-$[Pt(NH_3)_2(OH)_2(1\text{-MeC-}N3)_2]^{2+}$.[5a] There, the Pt^{IV} moves from N3 to the adjacent N4 site via an intermediate N3,N4 chelate. This migration is accompanied by a concomitant switch of a proton from N4 to N3. In contrast, in the present case Pt^{II} moves from N3 to N1, and there is a good chance that O2 assists in this process.

X-ray structure of heteronuclear derivative 4 of the mixed tautomer compound *trans*-[Pt(CH$_3$NH$_2$)$_2$(C-*N1*)(C-*N3*)] (3b): We have demonstrated in numerous cases that *trans*-$[Pta_2(1\text{-MeC-}N3)]^{2+}$ (a = NH_3 or CH_3NH_2) behaves as an excellent ligand for metal ions M, such as Pd^{II},[36] Cu^{II},[37] Ag^{I},[38] and Hg^{II},[16a, 16d] to produce heteronuclear complexes with the heterometal ions substituting protons of the exocyclic amino group. Strong dative Pt → M bonds are formed with the d^8 metal ion M = Pd^{II} and the d^9 metal ion M = Cu^{II}.[39] With this in mind, *trans*-$[Pt(CH_3NH_2)_2(CH\text{-}N3)_2](ClO_4)_2$ (**1a**) was mixed with $Cu(ClO_4)_2$ in aqueous NH_3 solution. To our surprise, a polymeric PtCu complex was isolated which contained the mixed linkage isomer species *trans*-$[Pt(CH_3NH_2)_2(C\text{-}N1)(C\text{-}N3)]$ (**3b**) as the central building block. We assume that **3b** is formed from **1b** in a linkage isomerization process as described above, although we cannot rigorously exclude the possibility that the starting material **1a** contained a small amount of **3a** as an impurity.

trans-$[Pt(CH_3NH_2)_2(N1\text{-C-}N3)(N3\text{-C-}N1)Cu(OH)]ClO_4 \cdot 1.2H_2O$ (**4**) consists of a 1D coordination polymer, in which *trans*-$[Pt(CH_3NH_2)_2(C\text{-}N1)(C\text{-}N3)]$ molecules are crosslinked by Cu^{II} ions through the still available N3 and N1 positions of the cytosine ligands. A complication arises from the coexistence of two bonding arrangements in the unit cell, which leads to a disorder of the cytosine amino group (Figure 9 and

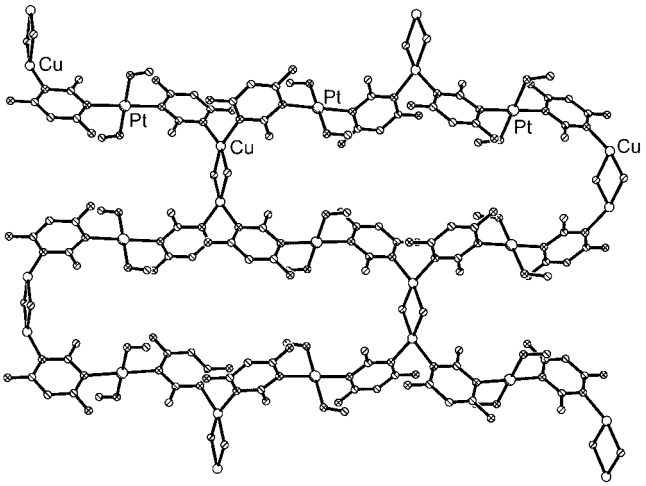

Figure 9. Section of polymeric arrangement of heteronuclear Cu derivative **4** of *trans*-$[Pt(CH_3NH_2)_2(C\text{-}N1)(C\text{-}N3)]$ (**3b**). The existence of two bonding arrangements in the unit cell leads to a superposition of exocyclic atoms of C with the NH_2 group disordered in *o* and *p* positions with respect to the ring N atom carrying the Pt.

the Experimental Section). In addition, Cu^{II} is bonded through two hydroxy bridges to another Cu^{II} center of another infinite strand, related by an inversion center. Pt–N bond lengths compare well with those of the cytosine complexes described, and the Cu–N bond length is also normal.[40] Conformation and metric parameters of the $Cu_2(OH)_2$ unit resemble those found in the bis(μ-hydroxo)-bis[bis(2-methylimidazole)copper(II)]$^{2+}$ cation.[41] Thus, the Cu–Cu distance of 2.946(3) Å in **4** is very close to that in the former complex (2.993(1) Å). The Cu centers have tetrahedrally distorted planar coordination spheres.

Conclusion

Cytosine exists in aqueous solution predominantly in the oxo-amino tautomer structure III, with the N1 position protonated and the N3 position unprotonated.[2a, 2c] The situation is reversed in the minor tautomer IV. Not unexpectedly, *trans*-$[(CH_3NH_2)_2Pt^{II}]$ reacts in water (weakly acidic pH) primarily

at the N3 position of tautomer III to give 1:1 and 1:2 complexes (**1**, **1a**). Interestingly, however, the mixed N3,N1 product **3a** forms in water to an extent incompatible with the low abundance of the rare tautomer. This observation, also confirmed for [(dien)Pt^{II}] binding to cytosine,[29] implies that metal species are, in principle, capable of "titrating out" a rare tautomer form from a solution containing a large excess of a preferred tautomer. Even though the specific example studied here—tautomerism of the parent nucleobase cytosine—is *not* of biological relevance, the phenomenon as such is potentially significant in metal-nucleobase chemistry and the topic of metal-related mispairing scenarios. A Hg^{II} complex of 9-methyladenine previously reported by us, [5f] in which the metal is coordinated to the exocyclic amino group and the proton is shifted to N1, represents an extreme case in this respect in that the rare imino tautomer (normal abundance $10^{-4}-10^{-5}$ relative to amino tautomer)[42] has been isolated on a preparative scale.

With regard to other aspects of this work, the following three features are pointed out. Firstly, there is the case of Pt^{II} migration from N3 to N1, hence linkage isomerization, under pH conditions in which N3-bound cytosine is deprotonated at N1. This indicates a higher thermodynamic stability of the Pt–N1 bond over the Pt–N3 bond in the neutral bis(cytosinato) complex of *trans*-[$(CH_3NH_2)_2Pt^{II}$]. Secondly, geometrical differences between platinated tautomers III and IV are essentially restricted to internal ring angles at N1, N3, C4, and C6. Thirdly, the major difference between the two metal-bonded cytosine tautomers refers to their acid/base behavior: Pt^{II} binding to N3 acidifies the proton at N1 by approximately 3.1 log units, from 12.15 in free cytosine to ≈9.1 (av.) in the N3 linkage isomer **1a**. In contrast, Pt^{II} binding to N1 acidifies the proton (of the metalated rare tautomer IV) at N3 by about 5–6 log units, from 12.15 to 6.07 or 7.09, respectively, in **2a**. This means that at a physiological pH, more than 50% of N1-platinated cytosine has its Watson–Crick sites available for base pairing with guanine.[43] Hoogsteen pairing is possible, in principle, also in acidic medium, with the N3 position protonated. We plan to study this aspect as well as potential applications resulting from it in more detail.

Experimental Section

Instrumentation: IR spectra (KBr pellets) were recorded on a Bruker IFs 113v FT spectrometer and Raman spectra on a Coderg T800 with argon (514.5 nm) or krypton laser (647.1 nm) excitation. ^1H NMR spectra were recorded with Bruker AC200 (200.13 MHz) or Bruker DRX400 (400 MHz) instruments. ^{195}Pt NMR spectra were recorded with a Bruker AC200 instrument (42.95 MHz, 5 mm tubes, ambient temperature). Chemical shifts are referenced to internal tetramethylammonium tetrafluoroborate (TMA) (^1H, $\delta = 3.18$ ppm versus TSP), the residual undeuterated DMSO signal ([D_6]DMSO; 2.50 ppm from TMS) (^1H) and external Na_2PtCl_6 (^{195}Pt), respectively. The two-dimensional E.COSY experiment was recorded on the DRX400 spectrometer in the phase-sensitive TPPI mode. Elemental analyses were performed with a Carlo Erba Model 1106 Strumentazione Element-Analyzer.

Starting compounds: Cytosine (CH) was obtained from Fluka. *trans*-[$Pt(CH_3NH_2)_2Cl_2$][44] and sodium cytosinate (NaC)[45] were prepared as previously described. DMF was dried over CaH_2 and stored over 4 Å molecular sieves.[46]

***trans*-[Pt(CH_3NH_2)$_2$(CH-*N3*)Cl]Cl·H_2O (1)**: A suspension of *trans*-[$Pt(CH_3NH_2)_2Cl_2$] (0.354 g, 1.08 mmol) in H_2O (120 mL) was stirred together with cytosine (120 mg, 1.08 mmol) and NaCl (196 mg, 3.36 mmol) for 3 d at 40 °C. The mixture was then reduced to a volume of 12 mL by rotary evaporation and subsequently concentrated further under a flow of N_2. After 7 d at 20 °C, a mixture of deep yellow crystals of *trans*-[$Pt(CH_3NH_2)_2Cl_2$] and pale yellow **1** had formed which were manually separated under a microscope. Crystals of **1** were washed with a minimum of ice water and allowed to dry in air. The yield was only 5%. Elemental analysis (%) for $C_6H_{15}N_5OCl_2Pt$ (439.2; anhydrate): C 16.41, H 3.44, N 15.94; found: C 16.3, H 3.4, N 16.0. X-ray crystallography revealed the presence of one molecule of water of crystallization.

***trans*-[Pt(CH_3NH_2)$_2$(CH-*N3*)$_2$](ClO_4)$_2$ (1a)**: *trans*-[$Pt(CH_3NH_2)_2Cl_2$] (1.64 g, 5 mmol) was suspended in H_2O (250 mL) and $AgClO_4 \cdot H_2O$ (2.229 g, 9.89 mmol) in H_2O (50 mL) was added. The suspension was stirred for 72 h at 40 °C with daylight excluded. After the solution had been cooled to room temperature, AgCl was filtered off and cytosine (1.113 g, 10 mmol) was added. The solution was then stirred at 80 °C for 5 h, evaporated to near dryness, and the precipitate filtered and recrystallized twice from 0.01N $HClO_4$. Crystals that formed were filtered off, briefly washed with cold water and dried in air. The compound was isolated in 32% yield. Elemental analysis (%) for $C_{10}H_{20}N_8O_{10}Cl_2Pt$ (678.3): C 17.71, H 2.97, N 16.52; found: C 17.7, H 2.9, N 16.5.

***trans*-[Pt(CH_3NH_2)$_2$(C-*N3*)$_2$]·2H_2O (1b)**: This was obtained by dissolving **1a** (600 mg, 0.885 mmol) in 0.055N LiOH (32 mL). The solution was concentrated to a volume of 15 mL. Slow evaporation at 4 °C gave colorless crystals of **1b**, which were filtered off, briefly washed with ice water and dried in air. The yield was 62%. Elemental analysis (%) for $C_{10}H_{22}N_8O_4Pt$ (513.4): C, 23.39, H 4.32, N 21.83; found: C 23.1, H 4.7, N 21.7.

***trans*-[Pt(CH_3NH_2)$_2$(CH-*N3*)$_2$](ClO_4)$_2$·2DMSO (1c)**: This was obtained by evaporation of a DMSO solution of **1a** (100 mg) in DMSO (2 mL). Within six months, a small amount of colorless cubes of **1c** appeared, which were filtered off and characterized by X-ray diffraction.

***trans*-[Pt(CH_3NH_2)$_2$(CH-*N1*)$_2$](NO_3)$_2$·3H_2O (2a)**: *trans*-[$Pt(CH_3NH_2)_2Cl_2$] (0.5 g, 1.52 mmol) was dissolved in dry DMF (30 mL) and stirred under nitrogen with $AgNO_3$ (0.5123 g, 3.01 mmol) at 40 °C for 3 d with daylight excluded. After the solution had been cooled to room temperature, AgCl was filtered off and NaC (0.3649 g, 2.74 mmol) was added. The suspension was stirred for 3 d at 40 °C under nitrogen. Then the solution was evaporated to dryness and the light yellow precipitate redissolved in H_2O (10 mL). The pH of the solution was brought to ≈7 by addition of 0.1N HNO_3. The mixture was cooled to 4 °C and left overnight. The precipitate that formed, presumably an adduct between **2a** and **2b**, was filtered off, briefly washed with small amounts of water and recrystallized twice from 0.01N HNO_3. The yield was 21%. Elemental analysis (%) for $C_{10}H_{26}N_{10}O_{11}Pt$ (657.5): C 18.27, H 3.99, N 21.30; found: C 18.4, H 4.0, N 21.3.

***trans*-[Pt(CH_3NH_2)$_2$(C-*N1*)$_2$]·2H_2O (2b)**: This was obtained by dissolving **2a** (100 mg) in 1N NaOH (3 mL) and evaporating the solution in a stream of nitrogen. Colorless crystals of **2b**, which formed within a few hours, were filtered off, briefly washed with water, and dried in air. The compound was isolated in 67% yield. Elemental analysis (%) for $C_{10}H_{22}N_8O_4Pt$ (513.4): C, 23.39, H 4.32, N 21.83; found: C 23.2, H 4.2, N 21.8.

***trans*-[Pt(CH_3NH_2)$_2$(CH-*N1*)(CH-*N3*)](ClO_4)$_2$ (3a)**: This was obtained as a by-product during the preparation of **1a**. Prior to recrystallization of **1a**, the ^1H NMR spectrum indicates the presence of this product (vide infra). Pure samples of **3a** could not be obtained. The neutral species *trans*-[$Pt(CH_3NH_2)_2$(C-*N1*)(C-*N3*)] (**3b**) was also detected only in solution (c.f., however, **4**).

***trans*-[Pt(CH_3NH_2)$_2$(*N1*-C-*N3*)(*N3*-C-*N1*)Cu(OH)]ClO_4·1.2H_2O (4)**: Compound **1a** (100 mg; not recrystallized from $HClO_4$, vide supra) was dissolved in a mixture of concentrated NH_3 (5 mL) and H_2O (15 mL), and $Cu(ClO_4)_2 \cdot H_2O$ (41 mg, 0.147 mmol) was added. The blue solution was slowly evaporated in a stream of nitrogen at ambient temperature. After filtering from some unidentified black precipitate, blue crystals (13 mg) appeared after 11 days. They were filtered off and dried in air. The composition of **4** was established by X-ray diffraction.

X-ray data collection, structure solutions, and refinements: Diffraction data of **1** were collected on a Rigaku AFC6S diffractometer with $Mo_{K\alpha}$ radiation ($\lambda = 0.71069$ Å). Calculations were performed on a VAX

0947-6539/02/0820-4690 $ 20.00+.50/0 *Chem. Eur. J.* **2002**, *8*, No. 20

station 3520 computer by applying the teXan 5.0 software.[47] Unit cell dimensions were determined by applying the setting angle of 25 high-angle reflections. Three standard reflections were monitored during the data collection; they showed no significant variance. The intensities were corrected for absorption by applying ψ scans of several reflections with the transmission factors in the range 0.60–1.00. The structure was solved by Patterson and Fourier techniques. Full-matrix least-squares refinement was carried out with anisotropic thermal parameters for all non-hydrogen atoms. The final difference map was essentially featureless.

Diffraction data of **1b**, **2a**, and **2b** were collected at room temperature on an Enraf-Nonius Mach3 diffractometer with graphite-monochromated $Mo_{K\alpha}$ radiation ($\lambda = 0.71069$ Å). The $\omega/2\Theta$ scan mode was employed with variable scan speed (1.2–4.1 °min^{-1}), and stationary background counts were recorded on each side of the reflection, the ratio of peak counting time vs. background counting time being 2:1. Three standard reflections measured every 100 data points showed no systematic variation in intensity. The data have been corrected for absorption, Lorentz, and polarization effects with the NRCVAX system.[48] An empirical absorption correction was carried out by means of azimuth (ψ) scans. For the data collection of **1a** and **1c**, an Enraf-Nonius KappaCCD[49] ($Mo_{K\alpha}$, $\lambda = 0.71069$ Å, graphite monochromator) was used. Sample-to-detector distances were 27.7 (**1a**) and 26.7 mm (**1c**), respectively. They covered the whole sphere of reciprocal space by measurement of 360 frames rotating about ω in steps of 1°. Exposure times were 7 s (**1a**) and 26 s (**1c**) per frame. Preliminary orientation matrices and unit cell parameters were obtained from the peaks of the first ten frames, respectively, and refined with the whole data set. Frames were integrated and corrected for Lorentz and polarization effects with DENZO.[50] The scaling as well as the global refinement of crystal parameters were performed by SCALEPACK.[50] Reflections, which were partly measured on previous and following frames, are used to scale these frames on each other. Merging of redundant reflections in part eliminates absorption effects and also considers a crystal decay, if present.

Structures of **1a**, **1b**, **1c**, **2a**, and **2b** were solved by standard Patterson methods[51] and refined by full-matrix least-squares based on F^2 with the SHELXTL-PLUS[52] and SHELXL-93 programs.[53] The scattering factors for the atoms were those given in the SHELXTL-PLUS program. Transmission factors were calculated with SHELXL-97.[54] All of the non-hydrogen atoms were refined anisotropically except for the disordered oxygen atoms of the anions in **1a** and **2a**. Hydrogen atoms could be found with difference Fourier synthesis and freely refined including water protons. Exceptions are the N1 proton in **1a**, all hydrogens in **1c**, and the methyl protons in **2a**, which were included in calculated positions and refined with isotropic displacement parameters according to the riding model. No protons were detectable for the half-occupied water molecule in **2a**.

X-ray measurements of **4** were carried out on a Quantum CCD detector using $Mo_{K\alpha}$ radiation ($\lambda = 0.71069$ Å). Calculations were performed by with the teXsan 1.7 crystallographic software package.[47] The data were collected with 0.25° scans with an exposure time of 104 s per image. Three standard reflections were monitored during the data collection showing no significant variance. The intensities were corrected for absorption by applying ψ scans of several reflections with the transmission factors in the range 0.65–1.00.

The structure of **4** was solved by Patterson and Fourier techniques. One of the Fourier maps revealed a peak with a height of ≈ 5 e Å^3 that was close to the C6 atom of the cytosine ligand. The existence of this peak led to the conclusion that the ligand is disordered between two orientations. In one of them, cytosine binds to Pt and Cu via the N1 and N3 atoms, respectively. In the other orientation, Pt is bonded to N3 and Cu to N1. There exists a significant overlap of the two orientations resulting in two locations of the amino N4 atom, labeled as N4a and N4b. The two positions were refined anisotropically with the population parameters of 0.5. The thermal vibration parameters of the methylamine ligand were high indicating a possible disorder. However, in spite of many efforts, this disorder could not be resolved. The perchlorate anion is disordered between two locations, refined as rigid bodies with isotropic thermal parameters. The solvent water molecules O4 and O6 are also disordered and were refined with isotropic temperature factors and the population parameters of 0.7 and 0.5, respectively. Full-matrix least-squares refinement yielded an R factor of 0.044 ($R_w = 0.065$). The final difference Fourier map showed a peak of 1.60 e Å^3 located near the disordered ClO_4^- ion.

CCDC-179624–CCDC-179630 contain the supplementary crystallographic data for this paper. These data can be obtained free of charge via www.ccdc.cam.ac.uk/conts/retrieving.html (or from the Cambridge Crystallographic Data Centre, 12 Union Road, Cambridge CB21EZ, UK; fax: (+44) 1223-336033; or deposit@ccdc.cam.uk).

Relevant X-ray data for all compounds are listed in Table 1.

Determination of acidity constants: The pK_a values of complexes **1a**, **2a**, and **3a,b** were determined by means of pH-dependent ^{1}H NMR measurements in D_2O (20 °C). Changes in chemical shifts of nonexchangeable protons in the complexes that result from the change in pD were evaluated with a nonlinear least-squares fit after Newton–Gauss, taking either one or two pK_a values into account.[55] The obtained acidity constants were then transformed to the values valid for water according to the literature.[56] For all calculations, only the signal of a single proton per complex could be evaluated, as the others could not be followed over the whole pD range because of the overlap with other signals; that is for **1a** (*ht*) H6, for **1a** (*hh*) H5, for **2a** H6, and for **3a** H6 were evaluated.

Acknowledgements

This work was supported by the Deutsche Forschungsgemeinschaft (DFG) and the Fonds der Chemischen Industrie (FCI). M.S. wishes to thank Dr. J. D. Ferrera and Dr. B. R. Vincent, Molecular Structure Corporation, the Woodland, TX, for their help with the data collection and structure determination of **4**.

[1] J. S. Kwiatkowski, B. Pullman, *Adv. Heterocycl. Chem.* **1975**, *18*, 199.
[2] a) A. R. Katritzky, A. Waring, *J. Chem. Soc.* **1963**, 3064; b) H. Morita, S. Nagakura, *Theor. Chim. Acta* **1968**, *11*, 279; c) J. Elguero, C. Marzin, A. R. Katritzky, P. Linda, *The Tautomerism of Heterocycles*, Academic Press, New York, **1976**, p. 159.
[3] C. Colominas, F. J. Luque, M. Orozco, *J. Am. Chem. Soc.* **1996**, *118*, 6811.
[4] M. Szczesniak, K. Szczepaniak, S. J. Kwiatkowski, K. Kubulat, W. B. Person, *J. Am. Chem. Soc.* **1988**, *110*, 8319.
[5] a) B. Lippert, H. Schöllhorn, U. Thewalt, J *Am. Chem. Soc.* **1986**, *108*, 6616; b) H. Schöllhorn, U. Thewalt, B. Lippert, *J. Am. Chem. Soc.* **1989**, *111*, 7213; c) O. Renn, B. Lippert, A. Albinati, *Inorg. Chim. Acta* **1991**, *190*, 285; d) B. Lippert, H. Schöllhorn, U. Thewalt, *Inorg. Chim. Acta* **1992**, *198–200*, 723; e) F. Pichierri, D. Holthenrich, E. Zangrando, B. Lippert, L. Randaccio, *J. Biol. Inorg. Chem.* **1996**, *1*, 439; f) F. Zamora, M. Kunsman, M. Sabat, B. Lippert, *Inorg. Chem.* **1997**, *36*, 1583; g) J. Müller, E. Zangrando, N. Pahlke, E. Freisinger, L. Randaccio, B. Lippert, *Chem. Eur. J.* **1998**, *4*, 397; h) J. Müller, F. Glahé, E. Freisinger, B. Lippert, B. *Inorg. Chem.* **1999**, *38*, 3160; i) J. Sponer, J. E. Sponer, L. Gorb, J. Leszczynski, B. Lippert, *J. Phys. Chem. A* **1999**, *103*, 11406.
[6] E. Zangrando, F. Pichierri, L. Randaccio, B. Lippert, *Coord. Chem. Rev.* **1996**, *156*, 275.
[7] D. T. Qui, M. Bagieu, *Acta Crystallogr. Sect. C* **1990**, *46*, 1645.
[8] a) M. Sundaralingam, J. A. Carrabine, *J. Mol. Biol.* **1971**, *61*, 287; b) T. J. Kistenmacher, D. J. Szalda, L. G. Marzilli, *Acta Crystallogr. Sect. B* **1975**, *31*, 2416; c) D. J. Szalda, L. G. Marzilli, T. J. Kistenmacher, *Inorg. Chem.* **1975**, *14*, 2076; d) A. Panfil, A. Terron, J. J. Fiol, M. Quiros, *Polyhedron* **1994**, *13*, 2513; e) M. Palaniandavar, I. Somasundaram, M. Lakshminarayanan, H. Manohar, *J. Chem. Soc. Dalton Trans.* **1996**, 1333.
[9] a) G. Cervantes, J. J. Fiol, A. Terron, V. Moreno, J. R. Alabart, M. Aquilo, M. Gomez, X. Solans, *Inorg. Chem.* **1990**, *29*, 5168; b) K. Aoki, M. A. Salam, *Inorg. Chim. Acta* **2001**, *316*, 50.
[10] G. D. Munno, S. Mauro, T. Pizzino, D. Viterbo, *J. Chem. Soc. Dalton Trans.* **1993**, 1113.
[11] A. L. Beauchamp, M. Simard, *Acta Crystallogr. Sect. A* **1984**, *40*, C67.
[12] a) J. E. Kickham, S. J. Loeb, *Inorg. Chem.* **1994**, *33*, 4351; b) J. E. Kickham, S. J. Loeb, S. L. Murphy, *J. Am. Chem. Soc.* **1993**, *115*, 7031.
[13] a) S. Jaworski, H. Schöllhorn, P. Eisenmann, U. Thewalt, B. Lippert, *Inorg. Chim. Acta* **1988**, *153*, 31; b) L. S. Hollis, A. R. Amundsen, E. W. Stern, *J. Med. Chem.* **1989**, *32*, 128.

  0947-6539/02/0820-4691 $ 20.00+.50/0

[14] For the compounds reported in ref. [11], no 3D structure diagrams are available. According to the authors, N1 coordination is also observed.
[15] a) H. Rauter, E. C. Hillgeris, B. Lippert, *Chem. Commun.* **1992**, 1385; b) H. Rauter, E. C. Hillgeris, A. Erxleben, B. Lippert, *J. Am. Chem. Soc.* **1994**, *116*, 616; c) H. Rauter, I. Mutikainen, M. Blomberg, C. J. L. Lock, P. Amo-Ochoa, E. Freisinger, L. Randaccio, E. Zangrando, E. Chiarparin, B. Lippert, *Angew. Chem.* **1997**, *109*, 1353; *Angew. Chem. Int. Ed. Engl.* **1997**, *36*, 1296.
[16] a) D. Holthenrich, I. Sóvágó, G. Fusch, A. Erxleben, E. C. Fusch, I. Rombeck, B. Lippert, *Z. Naturforsch. B* **1995**, *50*, 1767; b) A. Schreiber, O. Krizanovic, E. C. Fusch, B. Lippert, F. Lianza, A. Albinati, S. Hill, D. M. L. Goodgame, H. Stratemeier, M. A. Hitchman, *Inorg. Chem.* **1994**, *33*, 6101; c) O. Krizanovic, M. Sabat, R. Beyerle-Pfnür, B. Lippert, *J. Am. Chem. Soc.* **1993**, *115*, 5538; d) M. Krumm, E. Zangrando, L. Randaccio, S. Menzer, A. Danzmann, F. Holthenrich, B. Lippert, *Inorg. Chem.* **1993**, *32*, 2183; e) M. Krumm, E. Zangrando, L. Randaccio, S. Menzer, B. Lippert, *Inorg. Chem.* **1993**, *32*, 700.
[17] S. Metzger, A. Erxleben, B. Lippert, *J. Biol. Inorg. Chem.* **1997**, *2*, 256.
[18] R. J. McClure, B. M. Craven, *Acta Crystallogr. Sect. B* **1973**, *29*, 1234.
[19] The esd is calculated according to $\sigma = (\sigma_1^2 + \sigma_2^2)^{1/2}$ with σ_1 and σ_2 being the errors in bond lengths and angles which are compared.
[20] L. Clowney, S. C. Jain, A. R. Srinivasan, J. Westbrook, W. K. Olson, H. M. Berman, *J. Am. Chem. Soc.* **1996**, *118*, 509.
[21] a) B. L. Kindberg, E. L. Amma, *Acta Crystallogr.* **1975**, *B31*, 1492; b) K. Ogawa, K. Nishitani, T. Fujiwara, S. Shirotake, K.-I. Tomita, *Acta Crystallogr.* **1979**, *B35*, 965; c) P. E. Bourne, M. R. Taylor, *Acta Crystallogr. Sect. C* **1983**, *39*, 430.
[22] F. Fujinami, K. Ogawa, Y. Arakawa, S. Shirotake, S. Fujii, K.-I. Tomita, *Acta Crystallogr. Sect. B* **1979**, *35*, 968.
[23] J.-Y. Lallemand, J. Soulie, J.-C. Chottard, *Chem. Commun.* **1980**, 438.
[24] M. D. Reily, L. G. Marzilli, *J. Am. Chem. Soc.* **1986**, *108*, 6785.
[25] S. T. Sullivan, A. Ciccarese, F. P. Fanizzi, L. G. Marzilli, *Inorg. Chem.* **2001**, *40*, 455.
[26] G. Frommer, F. Lianza, A. Albinati, B. Lippert, *Inorg. Chem.* **1992**, *31*, 2434.
[27] a) B. Song, G. Feldmann, M. Bastian, B. Lippert, H. Sigel, *Inorg. Chim. Acta* **1995**, 235, 99; b) G. Schröder, B. Lippert, M. Sabat, C. J. L. Lock, R. Faggiani, B. Song, H. Sigel, *J. Chem. Soc. Dalton Trans.* **1995**, 3767.
[28] J. J. Christen, J. H. Rytting, R. M. Izatt, *J. Phys. Chem.* **1967**, *71*, 2700.
[29] W. Brüning, I. Ascaso, E. Freisinger, M. Sabat, B. Lippert, *Inorg. Chim. Acta*, in press.
[30] Differences in kinetics of complex formation (tautomer IV possibly reacting faster than III) and/or differences in reactivities of Pt−OH_2 and Pt−OH species are likely to be responsible. We have no indication of a linkage isomerization N3 → N1 at acidic pH and no evidence that excess CH converts one linkage isomer into another one.
[31] R. Stewart, M. G. Harris, *Can. J. Chem.* **1977**, *55*, 3807.
[32] K. Inagaki, Y. Kidani, *Bioinorg. Chem.* **1978**, *9*, 157.
[33] J. R. DeMember, F. A. Wallace, *J. Am. Chem. Soc.* **1975**, *97*, 6240.
[34] B. Lippert, *J. Raman Spectrosc.* **1979**, *8*, 274.
[35] C. F. Moreno Luque, E. Freisinger, R. Griesser, J. Ochocki, B. Lippert, H. Sigel, *J. Chem. Soc. Perkin Trans. 2*, **2001**, 2005.
[36] M. Krumm, B. Lippert, L. Randaccio, E. Zangrando, *J. Am. Chem. Soc.* **1991**, *113*, 5129.
[37] G. Fusch, E. C. Fusch, A. Erxleben, J. Hüttermann, H.-J. Scholl, B. Lippert, B. *Inorg. Chim. Acta* **1996**, *252*, 167.
[38] D. Holthenrich, M. Krumm, E. Zangrando, F. Pichierri, L. Randaccio, B. Lippert, *J. Chem. Soc. Dalton Trans.* **1995**, 3275.
[39] a) C. Mealli, F. Pichierri, L. Randaccio, E. Zangrando, M. Krumm, D. Holthenrich, B. Lippert, *Inorg. Chem.* **1995**, *34*, 3418; b) F. Pichierri, E. Chiarparin, E. Zangrando, L. Randaccio, D. Holthenrich, B. Lippert, *Inorg. Chim. Acta* **1997**, *264*, 109.
[40] T. J. Kistenmacher, D. J. Szalda, L. G. Marzilli, *Acta Crystallogr. Sect. B* **1975**, *31*, 2416.
[41] A. Bencini, D. Gatteschi, C. Zanchini, *Inorg. Chem.* **1985**, *24*, 700.
[42] R. V. Wolfenden, *J. Mol. Biol.* **1976**, *40*, 307.
[43] W. Brüning, R. K. O. Sigel, E. Freisinger, B. Lippert, *Angew. Chem.* **2001**, *113*, 3497; *Angew. Chem. Int. Ed.* **2001**, *40*, 3397.
[44] J. Arpalahti, B. Lippert, H. Schöllhorn, U. Thewalt, *Inorg. Chim. Acta* **1988**, *153*, 45.
[45] L. J. Sessler, D. Magda, H. Furuta, *J. Org. Chem.* **1992**, *57*, 818.
[46] *Organikum*, VEB Deutscher Verlag der Wissenschaften: Berlin, **1986**, p. 645.
[47] teXan 5.0: Single Crystal Structure Analysis Software. Molecular Structure Corporation, The Woodlands, TX 77381 (USA), **1989**.
[48] E. J. Gabe, Y. Le Page, J.-P. Charland, F. L. Lee, P. S. White, *J. Appl. Cryst.* **1989**, *22*, 384.
[49] NONIUS BV, KappaCCD package, Röntgenweg 1, P. O.Box 811, 2600 AV Delft (The Netherlands).
[50] Z. Otwinowsky, W. Minor, *Methods Enzymol.* **1996**, *276*, 307.
[51] G. M. Sheldrick, *Acta Crystallogr. Sect. A* **1990**, *46*, 467.
[52] Sheldrick, G. M., SHELXTL-PLUS (VMS), Siemens Analytical X-Ray Instruments, Inc.: Madison, WI, **1990**.
[53] G. M. Sheldrick, SHELXL-93, Program for crystal structure refinement, University of Göttingen (Germany) **1993**.
[54] G. M. Sheldrick, SHELXL-97, Program for the Refinement of Crystal Structures, University of Göttingen (Germany) **1997**.
[55] a) R. K. O. Sigel, E. Freisinger, B. Lippert, *J. Biol. Inorg. Chem.* **2000**, *5*, 287; b) R. K. O. Sigel, B. Lippert, *Chem. Commun.* **1999**, 2167; c) R. Tribolet, H. Sigel, *Eur. J. Biochem.* **1987**, *163*, 353.
[56] R. B. Martin, *Science* **1963**, *139*, 1198.

Received: February 19, 2002 [F3888]

  0947-6539/02/0820-4692 $ 20.00+.50/0